ELSEVIER

Contents lists available at ScienceDirect

Physics Letters A

www.elsevier.com/locate/pla



Doubly twisted Neimark-Sacker bifurcation and two coexisting two-dimensional tori



Munehisa Sekikawa a,*, Naohiko Inaba b

- ^a Department of Mechanical and Intelligent Engineering, Utsunomiya University, Utsunomiya 321-8585, Japan
- ^b Organization for the Strategic Coordination of Research and Intellectual Properties, Meiji University, Kawasaki 214-8571, Japan

ARTICLE INFO

Article history: Received 18 August 2015 Received in revised form 23 October 2015 Accepted 23 October 2015 Available online 28 October 2015 Communicated by C.R. Doering

Keywords: Quasiperiodic oscillations Invariant closed circles Two-dimensional tori Neimark–Sacker bifurcations Lyapunov analysis

ABSTRACT

We discuss a complicated bifurcation structure involving several quasiperiodic bifurcations generated in a three-coupled delayed logistic map where a doubly twisted Neimark–Sacker bifurcation causes a transition from two coexisting periodic attractors to two coexisting invariant closed circles (ICCs) corresponding to two two-dimensional tori in a vector field. Such bifurcation structures are observed in Arnol'd tongues. Lyapunov and bifurcation analyses suggest that the two coexisting ICCs and the two coexisting periodic solutions almost overlap in the two-parameter bifurcation diagram.

© 2015 Elsevier B.V. All rights reserved.

1. Introduction

Quasiperiodic bifurcations have recently attracted considerable attention [1–13,15,14,16–32]. They mainly include quasiperiodic Neimark–Sacker (QNS) bifurcations and quasiperiodic saddlenode (QSN) bifurcations in maps and flows [31]. Three- or higher dimensional quasiperiodic oscillations generate extremely complex bifurcation structures denoted as Arnol'd resonance webs by Broer et al. [1] where web-like partial entrainment regions extend in numerous directions [1]. Arnol'd resonance webs in discrete dynamics [1,6,9,15,14,23,32] and ordinary differential equations [5,8,22] have been extensively studied. The pioneering work of partial synchronizations by Linsay and Cumming was based on detailed circuit experiments [2]. They introduced the term "fractal devil's cobweb." Moreover, Baesens et al. studied a family of torus maps that captures the essence of the partial synchronization and introduced the term "mode-locking web" [3].

The main focus in studying Arnol'd resonance webs is to find how a conventional Arnol'd tongue transits to a high-dimensional Arnol'd resonance tongue near a QNS bifurcation curve. Note that the QNS bifurcations are also denoted as quasiperiodic Hopf (QH) bifurcations [10]. Takens and Wagener analyzed such bifurcation transitions using bifurcation analysis [27]. Moreover, Kuznetsov and Meijer investigated the codimension-two bifurcation points

denoted as flip-Neimark–Sacker (flip-NS) and double NS bifurcations, and conducted Lyapunov analysis in simple maps [28]. The simplest transition may be that of a conventional Arnol'd tongue bifurcating to a two-dimensional torus Arnol'd tongue via a Neimark–Sacker (NS) bifurcation [23]. A more complex transition was reported by Broer et al. [9].

Our previous studies showed that the two- and three-coupled delayed logistic maps generate typical bifurcations such as QNS bifurcations and QSN bifurcations. Anishchenko et al. showed that the QSN bifurcation from a stable two-dimensional torus to a three-dimensional torus occurs because of the saddle-node bifurcation of the stable two-dimensional torus and saddle twodimensional torus [12,13]. In our previous studies [14,15], we showed that the stable invariant two-torus exists due to the saddle-node (SN) bifurcation of a stable invariant one-torus and saddle invariant one-torus in the two-coupled delayed logistic map [14], and the stable invariant three-torus exists due to the SN bifurcation of a stable invariant two-torus and saddle invariant two-torus in the three-coupled delayed logistic map [15]. These results strongly suggest that a stable (n + 1)-dimensional torus is generated owing to the SN bifurcation of a stable *n*-dimensional torus and saddle n-dimensional torus in a vector field. Such bifurcation structures are noteworthy. The coupled delayed-logistic maps capture the essence of the underlying mechanism of the quasiperiodic bifurcations.

In this study, we present a complex bifurcation transition from a conventional Arnol'd tongue to an invariant one-torus Arnol'd tongue [14] generated in a three-coupled delayed logistic map,

^{*} Corresponding author.

E-mail address: sekikawa@cc.utsunomiya-u.ac.jp (M. Sekikawa).

Table 1 Solutions and phenomena, where λ_i is the *i*-th Lyapunov exponent.

Мар	Lyapunov spectra	Vector fields
Periodic solution (IT ₀)	$\lambda_1 < 0$	Limit cycle
Invariant one-torus (IT_1)	$\lambda_1=0, \lambda_2<0$	Two-dimensional
(or ICC)		torus
Invariant two-torus (IT ₂)	$\lambda_1=\lambda_2=0, \lambda_3<0$	Three-dimensional
		torus
Invariant three-torus (IT ₃)	$\lambda_1=\lambda_2=\lambda_3=0, \lambda_4<0$	Four-dimensional
		torus

where an invariant one-torus corresponds to a two-dimensional torus in a vector field. The invariant one-torus is often called an invariant closed curve (ICC) in discrete time dynamics [23]. We discovered that two periodic points with a period of 93 coexist in the Arnol'd tongue; moreover, the two periodic solutions bifurcate to two coexisting invariant one-tori in the Arnol'd tongue that comprises 93 ICCs via two successive NS bifurcations. The bifurcation structure is very complicated because two invariant one-tori coexist although they are in close proximity in the state space. We conduct a bifurcation analysis of this bifurcation structure and show that a doubly twisted NS bifurcation curve causes such a transition near a ONS bifurcation, and also generates double flip-NS bifurcation. The detailed explanation for the derivation of the two coexisting periodic solutions is given in the Appendix. We assert that the two coexisting attractors are linked through saddle solutions.

2. Results

We conduct a Lyapunov analysis of the three-coupled delayed logistic map represented by the following equation.

$$F(x_{n}, y_{n}, z_{n}, w_{n}, u_{n}, v_{n}) : x_{n+1} = y_{n},$$

$$y_{n+1} = B_{1}y_{n}(1 - x_{n}) + \varepsilon_{1}w_{n} + \varepsilon_{2}v_{n},$$

$$z_{n+1} = w_{n},$$

$$w_{n+1} = B_{2}w_{n}(1 - z_{n}) + \varepsilon_{3}v_{n} + \varepsilon_{4}y_{n},$$

$$u_{n+1} = v_{n},$$

$$v_{n+1} = B_{3}v_{n}(1 - u_{n}) + \varepsilon_{5}y_{n} + \varepsilon_{6}w_{n},$$
(1)

where $\varepsilon_1, \varepsilon_2, \varepsilon_3, \varepsilon_4, \varepsilon_5$, and ε_6 are coupling parameters. Because the single delayed logistic map generates an invariant one-torus via an NS bifurcation, the three-coupled delayed logistic map can generate an invariant three-torus with three zero Lyapunov exponents. Throughout the discussion, we use

$$\varepsilon_1 = 0.01, \ \varepsilon_2 = 0.002, \ \varepsilon_3 = 0.001, \ \varepsilon_4 = 0.02,$$

$$\varepsilon_5 = 0.01, \ \varepsilon_6 = 0.01, \ B_3 = 2.05,$$
(2)

and allow parameters B_1 and B_2 to vary. The six Lyapunov exponents $(\lambda_1, \lambda_2, \ldots, \lambda_6)$ in Eq. (1) are calculated using the procedure presented by Shimada and Nagashima [33]. To distinguish the QNS bifurcation from an invariant one-torus to an invariant two-torus and the QNS bifurcation from an invariant two-torus to an invariant three-torus, we denote the latter as QNS₂ bifurcation. Similarly, we denote the QSN bifurcation from an invariant two-torus to an invariant three-torus as QSN₂ bifurcation.

In this study, we regard a Lyapunov exponent as exact zero if the following condition is satisfied.

$$\lambda_i < 10/N, \tag{3}$$

where N is the number of iterations. According to our numerical calculation, the fourth Lyapunov exponent λ_4 is always negative. The terms and their abbreviations are listed in Tables 1 and 2. Fig. 1 shows a two-parameter Lyapunov diagram near the QNS₂ bi-

Table 2 Classification of bifurcations.

Bifurcations	Abbreviations
Neimark-Sacker bifurcation	NS
Saddle-node bifurcation	SN
Quasiperiodic Neimark-Sacker bifurcation from IT ₁ to IT ₂	QNS
(or Quasiperiodic Hopf bifurcation from IT ₁ to IT ₂)	(or QH)
Quasiperiodic saddle-node bifurcation from IT ₁ to IT ₂	QSN
Quasiperiodic Neimark-Sacker bifurcation from IT ₂ to IT ₃	QNS_2
(or Quasiperiodic Hopf bifurcation from IT_2 to IT_3)	(or QH ₂)
Quasiperiodic saddle-node bifurcation from IT ₂ to IT ₃	QSN ₂

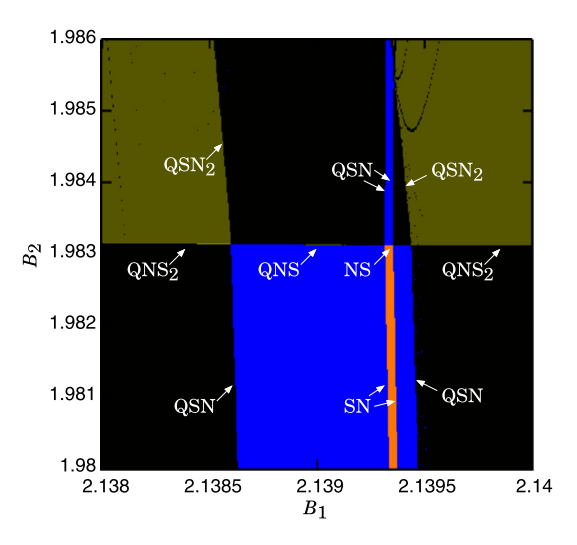


Fig. 1. Two-parameter Lyapunov diagram near the QNS $_2$ bifurcation curve (M = 10,000,000 and N = 10,000,000 with a grid mesh of 1000×1000). (For interpretation of the references to color in this figure, the reader is referred to the web version of this article.)

furcation curve. In Fig. 1, the regions generating periodic solutions, invariant one-tori, invariant two-tori, and invariant three-tori are shown in orange, blue, black, and dark green, respectively. Chaos is not observed in the parameter range of this diagram. As seen in Fig. 1, an invariant one-torus Arnol'd tongue bifurcates to an invariant two-torus Arnol'd tongue via a QNS bifurcation. Furthermore, a conventional Arnol'd tongue is clearly observed inside them and transits to an invariant one-torus Arnol'd tongue through an NS bifurcation.

We focus on the bifurcation structures of the transition from the conventional Arnol'd tongue to the invariant one-torus Arnol'd tongue. At first glance, this transition appears to be a simple NS bifurcation similar to that presented in Ref. [23]. However, the bifurcation analysis clarifies that the two solutions coexist in the conventional Arnol'd tongue and invariant one-torus Arnol'd tongue. To the best of our knowledge, such complex structure has not been reported to date.

Fig. 2 shows a magnified view of Fig. 1. The NS bifurcation curve and four (SN) bifurcation curves are explained below. The two coexisting periodic attractors with a period of 93 obtained at P in Fig. 2 are shown in Figs. 3(a.1) and 3(a.2), respectively. Figs. 3(a.1) and 3(a.2) are magnified and shown in Figs. 3(b.1) and 3(b.2), respectively. It is recognized from Fig. 3 that these are different attractors. The procedure for obtaining these two periodic solutions is explained in Appendix A. In addition, by tracing the above-mentioned parameter values above from P in the diagram, the two coexisting periodic solutions bifurcate to two coexisting invariant one-tori. The two coexisting invariant one-tori are shown in Figs. 4(a.1) and 4(a.2) and magnified in Figs. 4(b.1) and 4(b.2), respectively.

Download English Version:

https://daneshyari.com/en/article/1859034

Download Persian Version:

https://daneshyari.com/article/1859034

Daneshyari.com